Ultra high speed optical transmission using subcarrier-multiplexed four-dimensional LDPC-coded modulation

Hussam G. Batshon[1,*], Ivan Djordjevic[1], and Ted Schmidt[2]

[1] *Department of Electrical and Computer Engineering, University of Arizona, 1230 E. Speedway Blvd., Tucson, AZ 85721, USA*

[2] *Opnext Subsystems, 151 Albright Way, Los Gatos, CA 95032, USA*

**hbatshon@email.arizona,.edu*

Abstract: We propose a subcarrier-multiplexed four-dimensional LDPC bit-interleaved coded modulation scheme that is capable of achieving beyond 480 Gb/s single-channel transmission rate over optical channels. Subcarrier-multiplexed four-dimensional LDPC coded modulation scheme outperforms the corresponding dual polarization schemes by up to 4.6 dB in OSNR at BER 10^{-8}.

OCIS codes: (060.0060) Fiber optics and optical communications; (060.1660) Coherent communications; (060.4080) Modulation; (999.9999) Four-dimensional modulation; (999.9999) Forward error correction; (999.9999) Low-density parity-check (LDPC) codes; (999.9999) Subcarrier Multiplexing; (999.9999) Coded modulation.

References and links

1. J. Hong and T. Schmidt, "40G and 100G modules enable next generation networks," Communications and Photonics conference and Exhibition, 2009 ACP 2009, 1–2 (2009).
2. H. G. Batshon, I. B. Djordjevic, L. Xu, and T. Wang, "Multidimensional LDPC-Coded Modulation for Beyond 400 Gb/s per Wavelength Transmission," IEEE Photon. Technol. **21**(16), 1139–1141 (2009).
3. M. Karlsson and E. Agrell, "Which is the most power-efficient modulation format in optical links?" Opt. Express **17**(13), 10814–10819 (2009).
4. H. Bülow, "Polarization QAM Modulation (POL-QAM) for Coherent Detection Schemes," Opt. Fiber Commun. OWG2 (2009).
5. I. B. Djordjevic, M. Cvijetic, L. Xu, and T. Wang, "Proposal for beyond 100 Gb/s optical transmission based on bit-interleaved LDPC-coded modulation," IEEE Photon. Technol. Lett. **19**(12), 874–876 (2007).
6. S. ten Brink, J. Speidel, and R. H. Yan, "Iterative demapping for QPSK modulation," Electron. Lett. **34**(15), 1459–1460 (1998).
7. L. L. Minkov, I. B. Djordjevic, L. Xu, and T. Wang, "PMD compensation in polarization multiplexed multilevel modulations by turbo equalization," IEEE Photon. Technol. Lett. **21**(23), 1773–1775 (2009).

1. Introduction

Coherent systems with polarization multiplexing in optical communications are becoming more attractive alternatives to the conventional systems for their potential of realizing higher transmission rates. Different research groups are coming up with approaches to keep up with the increasing demands of the communication systems stemming from the dramatic increase in the amount and quality of the data-centric services and multimedia [1].

In [2], we discuss a generic multidimensional LDPC coded modulations that demonstrates improvements over the two-dimensional constellations. In this paper, we propose the subcarrier multiplexed four-dimensional LDPC bit-interleaved coded modulation (BICM) as a scheme capable of achieving 480 Gb/s and beyond per wavelength optical transmission using commercially available components operating at 50 Giga symbols/s (50 GS/s). Using BICM the system can achieve an effective aggregate rate greater than that of the individual components. Notice that we denote by BICM the modulation scheme described in [5]. As opposed to most coherent systems that employ polarization multiplexing to reduce the symbol rate and end up in suboptimal performance, this scheme leverages coding of symbols between the polarization states to improve performance. Moreover, the proposed scheme improves the

#133191 - $15.00 USD Received 11 Aug 2010; revised 29 Aug 2010; accepted 1 Sep 2010; published 10 Sep 2010

system performance by adding another degree of freedom, hence increasing the Euclidean distance in four-dimensional (4-D) constellations for the same symbol energy, in addition to the 4-D mapping and demapping. The mapper maps the incoming bits to four coordinates instead of using polarization multiplexing and two independent mappers. The demapper on the other hand can compensate for nonlinear polarization mode dispersion (PMD) effects [7], whereas corresponding polarization multiplexing scheme cannot. Previous work [3], [4] has proposed polarization multiplexing and coding between states, meanwhile the scheme presented in this paper is capable of exploiting the full potential of the four dimensions. As opposed to conventional polarization multiplexed quadrature amplitude modulation (PolMux-QAM) systems that multiplex two independent 2-D streams the presented scheme is a modulation scheme and the data stream at the output of the modulator is 4-D.

2. Subcarrier multiplexed four-dimensional LDPC-coded modulation

The transmission system of the subcarrier multiplexed (SM) 4-D modulation scheme is composed of two 4-D subsystems. The block diagram of this system is shown in Fig. 1. As shown in the figure, $2 \times m$ input bit streams from different information sources are divided into two groups of *m* streams per group. The *m* streams of each group are used as input to a 4-D transmitter. Each transmitter is assigned a unique subcarrier, this subcarrier is used to modulate the 4-D signal. The outputs of the two 4-D transmitters are then forwarded to a power combiner then to the optical channel. At the receiver side, the signal is split into two branches and forwarded to the two 4-D receivers.

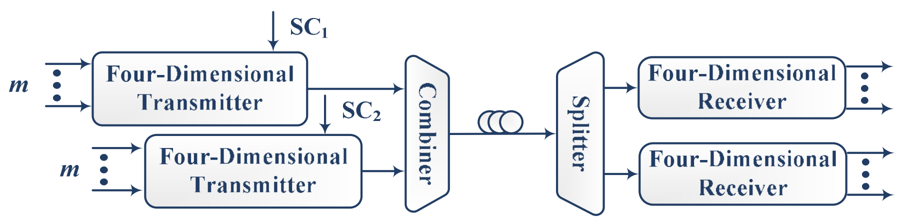

Fig. 1. Subcarrier-multiplexed four-dimensional LDPC-coded modulation: System block diagram.

After explaining the SM 4-D system, we turn our focus to the 4-D system configuration. The transmitter of the 4-D system, shown in Fig. 2(a) accepts the input of the *m* bit streams coming from the *m* input information sources into a set of identical LDPC encoders of code rate *k/n*. (*k* represents the number of information bits that the encoder accepts at a given time to output a codeword of length *n*). The encoded data from these branches is forwarded to an $m \times n$ block interleaver where it is written row-wise and read column-wise to a single bit stream. At a time instant *i*, the mapper reads *m* bits to determine the corresponding 2^m-ary signal constellation point. The mapper is based on a simple look-up table (LUT) with 2^m memory locations. It follows the mapping rule to select the output voltages needed to control the modulator. The output of the mapper is in the form $\left(f_{1,i}, f_{2,i}, f_{3,i}, f_{4,i}\right)$. These voltages and hence the mapping rule change according to the type of modulator used. In this paper, we present two equivalent modulators, the in-phase/quadrature (I/Q) modulator that is represented by the Cartesian coordinates, and the amplitude/phase (A/P) modulator that is represented in Polar coordinates. In the I/Q representation, the mapper uses a look-up table to map the received *m* bits into the signal point, $s_i = \left(I_{x,i}, Q_{x,i}, I_{y,i}, Q_{y,i}\right)$. In s_i, *I* refers to the in-phase component while the *Q* refers to the quadrature component. *x* and *y* refer to the x-polarization and the y-polarization, respectively. The A/P representation, on the other hand, maps the received *m* bits into the signal point $s_i = \left(\left|s_{x,i}\right|, \theta_{x,i}, \left|s_{y,i}\right|, \theta_{y,i}\right)$ where $|s|$ and θ refer to the amplitude, and the phase for the signal at a given polarization, respectively. These two representations can be written in a vector form as shown in (1).

#133191 - $15.00 USD Received 11 Aug 2010; revised 29 Aug 2010; accepted 1 Sep 2010; published 10 Sep 2010

$$s_i = \begin{pmatrix} \Re(E_{x,i}) \\ \Im(E_{x,i}) \\ \Re(E_{y,i}) \\ \Im(E_{y,i}) \end{pmatrix} = \begin{pmatrix} I_{x,i} \\ Q_{x,i} \\ I_{y,i} \\ Q_{y,i} \end{pmatrix} = \begin{pmatrix} |s_{x,i}|\cos\theta_{x,i} \\ |s_{x,i}|\sin\theta_{x,i} \\ |s_{y,i}|\cos\theta_{y,i} \\ |s_{y,i}|\sin\theta_{y,i} \end{pmatrix} \tag{1}$$

Figure 2(b) shows the conventional PolMux-QAM modulator using nested Mach-Zehnder modulators (MZM). Figure 2(c) on the other hand, shows the receiver of the 4-D system. At the receiver side, the optical signal is split into two orthogonal polarizations using the polarization beam splitter (PBS) and is used as input into two coherent detectors. The coherent detectors provide the estimated in-phase and quadrature information for both polarizations to be used in the turbo-like decoding algorithm explained below. The outputs of the detectors are demodulated by the subcarrier specified for the corresponding 4-D receiver then sampled at the symbol rate. The output samples are forwarded to the a posteriori probability (APP) demapper and a bit log-likelihood ratios (LLRs) calculator in order to provide the bit LLRs required for iterative LDPC decoding. The APP demapper calculates the symbol log-likelihood ratios (LLRs) using the following equation,

$$\lambda(s_i) = \log\left[\frac{P(s_i = s_0 | r_i)}{P(s_i \neq s_0 | r_i)}\right] \tag{2}$$

where $P(\boldsymbol{s}_i|\boldsymbol{r}_i)$ is determined by Bayes' rule as:

$$P(s_i|r_i) = \frac{P(r_i|s_i)P(s_i)}{\sum_{s'} P(r_i|s_i')P(s_i')} \tag{3}$$

The bit LLRs calculator on the other hand calculates the bit LLRs from the Symbol LLRs, as follows,

$$L(\hat{v}_j) = \log\left[\frac{\sum_{s_i:v_j=0} \exp(\lambda(s_i))}{\sum_{s_i:v_j=1} \exp(\lambda(s_i))}\right] \tag{4}$$

In the above equations s_i denotes the transmitted signal constellation point, r_i denotes the received constellation point, where $\boldsymbol{s_0}$ denotes the referent constellation point. $P(r_i \mid s_i)$, on the other hand, denotes the conditional probability, and $P(s)$ is the a priori symbol probability, while $\hat{v}_j$ for $j \in \{0,1,\cdots,n-1\}$ is the *j*th bit of the codeword *v*. The bit LLRs are forwarded to LDPC decoders, which provide extrinsic bit LLRs for demapper and are used as inputs to (3) as prior information.

The turbo-like decoding process is used to reduce the number of iterations required by the LDPC decoder to reach convergence, and it is performed as follows. After the bit LLRs are calculated, the extrinsic LLRs of the demapper are forwarded to the LDPC decoder as the a priori probabilities to be used in the LDPC decoding process. The resulting extrinsic information of the LDPC decoder are sent back to the APP demapper to be used as the a priori reliabilities again. The process of iterating the extrinsic information between the APP demapper and the LDPC decoder is denoted in this paper by the *outer iteration*. In the turbo-like decoding algorithm, the outer back and forth iterations are repeated until convergence is

#133191 - $15.00 USD Received 11 Aug 2010; revised 29 Aug 2010; accepted 1 Sep 2010; published 10 Sep 2010

achieved unless a predefined number of iterations is reached. Once the iterations stop, the LDPC decoders will yield the decoded data to the m outputs.

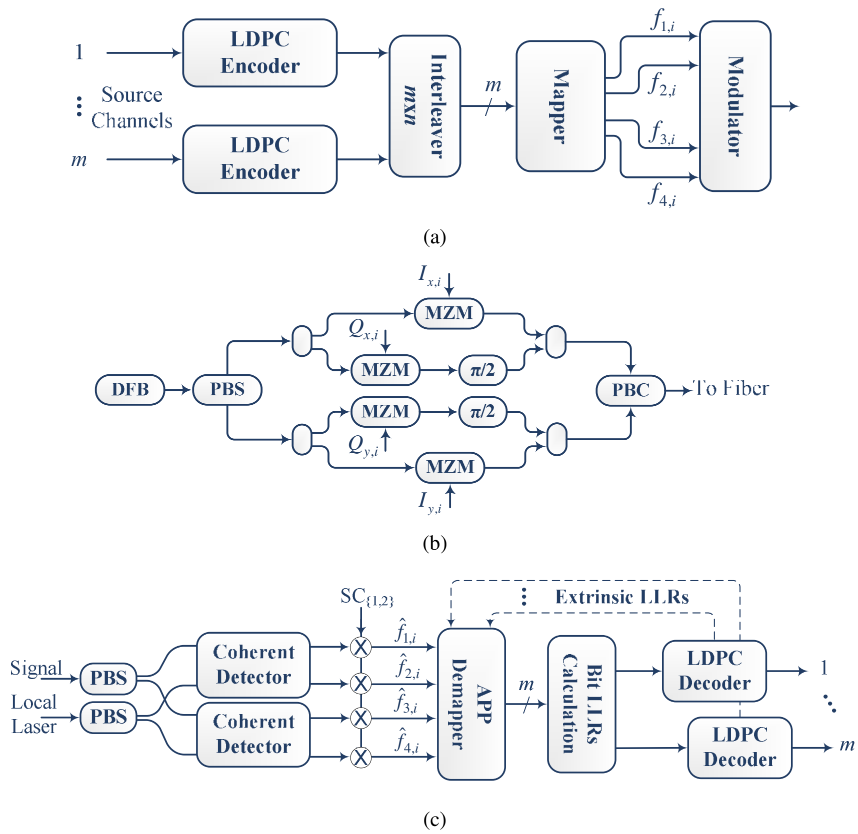

Fig. 2. Block diagram of the four-dimensional: (a) transmitter, (b) I/Q modulator and (c) receiver.

As mentioned in the Introduction, the LDPC codes used in this scheme are structured LDPC codes for their attractive properties. The codes used are selected based on the extrinsic information transfer (EXIT) charts analysis [5,6], as they have to guarantee convergence in the turbo-like iterative process between the APP demapper and the LDPC decoders. The iterative demapping scheme used in this paper is a generalization of the scheme invented by ten Brink.

3. Simulation setup and numerical results

The system is verified over an ASE noise dominated channel for different scenarios. The simulations are performed on a linear channel model, at symbol rate of 50 GS/s, for 25 inner iterations, and 3 outer iterations. Different signal constellations are observed for both the proposed scheme and the PolMux-M-QAM, where M represents the number of constellation points per polarization. For the PolMux-M-QAM, each polarization is modulated with the conventional QAM from literature. The following signal constellations are observed: 16-SM-4D constellation, and its corresponding PolMux-16-QAM, 32-SM-4D constellation and its corresponding PolMux-32-QAM, in addition to the 64-SM-4D constellation and its corresponding PolMux-64-QAM. In these simulations, correspondence is based on the number of bits per symbol, all the different constellations for both formats are verified over the system in Fig. 2.

#133191 - $15.00 USD   Received 11 Aug 2010; revised 29 Aug 2010; accepted 1 Sep 2010; published 10 Sep 2010

Table 1. Mapping rule look-up table for 16-4D.

Interleaver output	$\{I_x,Q_x,I_y,Q_y\}$
0000	{-1,-1,-1,-1}
0001	{-1,-1,-1,1}
0010	{-1,-1,1,-1}
0011	{-1,-1,1,1}
0100	{-1,1,-1,-1}
0101	{-1,1,-1,1}
0110	{-1,1,1,-1}
0111	{-1,1,1,1}
1000	{1,-1,-1,-1}
1001	{1,-1,-1,1}
1010	{1,-1,1,-1}
1011	{1,-1,1,1}
1100	{1,1,-1,-1}
1101	{1,1,-1,1}
1110	{1,1,1,-1}
1111	{1,1,1,1}

Table 2. Mapping rule look-up table for 32-4D.

Interleaver output	$\{I_x,Q_x,I_y,Q_y\}$	***Interleaver output***	$\{I_x,Q_x,I_y,Q_y\}$
00000	{-½,-½,-½,-½}	10000	{0,0,0,-1}
00001	{-½,-½,-½,½}	10001	{0,0,0,1}
00010	{-½,-½,½,-½}	10010	{0,0,-1,0}
00011	{-½,-½,½,½}	10011	{0,0,1,0}
00100	{-½,½,-½,-½}	10100	{0,-1,0,0}
00101	{-½,½,-½,½}	10101	{0,1,0,0}
00110	{-½,½,½,-½}	10110	{-1,0,0,0}
00111	{-½,½,½,½}	10111	{1,0,0,0}
01000	{½,-½,-½,-½}	11000	{-1,0,0,-1}
01001	{½,-½,-½,½}	11001	{-1,0,0,1}
01010	{½,-½,½,-½}	11010	{1,0,0,-1}
01011	{½,-½,½,½}	11011	{1,0,0,1}
01100	{½,½,-½,-½}	11100	{0,-1,-1,0}
01101	{½,½,-½,½}	11101	{0,-1,1,0}
01110	{½,½,½,-½}	11110	{0,1,-1,0}
01111	{½,½,½,½}	11111	{0, 1,1,0}

For the 16-4D constellation, the mapper maps the 2^m possible points into the different combinations of the 4-D vectors (± 1, ± 1, ± 1, ± 1), these coordinates form the vertices of a tesseract (a regular octachoron). Meanwhile, for the 32-4D constellation, 16 out of the 32 possible points are mapped to the different combinations of the 4-D vectors (± ½, ± ½, ± ½, ± ½), 8 out of the 32 points are mapped to the different combinations of (± 1,0,0,0) and its permutations, 4 out of the 32 points are mapped to the different combinations of (± 1,0,0, ± 1), and the remaining 4 are mapped the different combinations of (0, ± 1, ± 1,0). On the other hand, for the 64-4D constellation, the 64 possible points are mapped to eight of the twelve non-disjoint even permutations of $\frac{1}{2}\left(\pm 1, \pm\varphi, \pm \frac{1}{\varphi}, 0\right)$, where $\varphi = \left(1+\sqrt{5}\right)/2$ is the golden ratio. The mapping rule lookup-table for the 16-4D constellation and the 32-4D constellation are shown in Tables 1 and 2 respectively.

Figure 3 shows a comparison of the BER performance among the LDPC coded PolMux-QAM, and SM-4D LPDC-coded modulation schemes. The LDPC(16935,13550) code used for these simulations is a structured LDPC [5] code of code rate 0.8 and of girth 10, where girth is defined as the length of the shortest cycle in the Tanner graph representation of the LDPC code. The improvement of the SM-4D scheme is reported at BER of 10^{-8} as follows: 16-SM-4D outperforms the 16-PolMux-QAM that utilizes both polarizations and has the same aggregate rate of by 4 dB. On the other hand, 32-SM-4D outperforms the 32-PolMux-QAM

#133191 - $15.00 USD Received 11 Aug 2010; revised 29 Aug 2010; accepted 1 Sep 2010; published 10 Sep 2010

that utilizes both polarizations and has the same aggregate rate of by 4.4 dB. At last, 64-SM-4D outperforms the corresponding 64-PolMux-QAM by 4.6 dB.

The aggregate rates for the presented modulation formats are $2 \times 4 \times 50 \times 0.8 = 320$ Gb/s for the16-SM-4D and PolMux-16-QAM, at a symbol rate of 50 GS/s while it is $2 \times 5 \times 50 \times 0.8 = 400$ Gb/s for the 32-SM-4D and PolMux-32-QAM, and $2 \times 6 \times 50 \times 0.8 = 480$ Gb/s for the 64-SM-4D and PolMux-64-QAM.

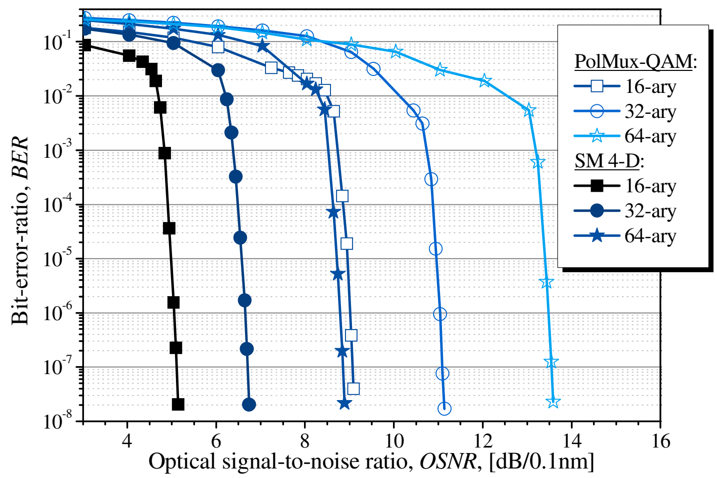

Fig. 3. BER performance of the proposed scheme in comparison with PolMux QAM LDPC-coded modulation.

4. Conclusion

Subcarrier multiplexed 4-D LDPC BICM is proposed in this paper as a modulation scheme that can achieve up to 480 Gb/s transmission rate per wavelength using multiple components of 50 GS/s working in parallel. The proposed scheme is capable of outperforming its PolMux counterpart by up to 4.6 dB in OSNR at BER of 10^{-8} utilizing subcarrier multiplexing. This scheme is suitable for high speed transmission systems operating at rates 400 Gb/s and higher.

Acknowledgments

This work was supported in part the National Science Foundation (NSF) under Grants CCF-0952711 and ECCS-0725405.

#133191 - $15.00 USD Received 11 Aug 2010; revised 29 Aug 2010; accepted 1 Sep 2010; published 10 Sep 2010